



ALMA MATER STUDIORUM
UNIVERSITÀ DI BOLOGNA

ARCHIVIO ISTITUZIONALE
DELLA RICERCA

Alma Mater Studiorum Università di Bologna Archivio istituzionale della ricerca

The relationship between tibiofemoral geometry and musculoskeletal function during normal activity

This is the final peer-reviewed author's accepted manuscript (postprint) of the following publication:

Published Version:

Martelli S., Sancisi N., Conconi M., Pandy M.G., Kersh M.E., Parenti-Castelli V., et al. (2020). The relationship between tibiofemoral geometry and musculoskeletal function during normal activity. *GAIT & POSTURE*, 80, 374-382 [10.1016/j.gaitpost.2020.06.022].

Availability:

This version is available at: <https://hdl.handle.net/11585/807782> since: 2024-05-09

Published:

DOI: <http://doi.org/10.1016/j.gaitpost.2020.06.022>

Terms of use:

Some rights reserved. The terms and conditions for the reuse of this version of the manuscript are specified in the publishing policy. For all terms of use and more information see the publisher's website.

This item was downloaded from IRIS Università di Bologna (<https://cris.unibo.it/>).
When citing, please refer to the published version.

(Article begins on next page)

Abstract

Background

The effect of tibiofemoral geometry on musculoskeletal function is important to movement biomechanics.

Research question

We hypothesised that tibiofemoral geometry determines tibiofemoral motion and musculoskeletal function. We then aimed at 1) modelling tibiofemoral motion during normal activity as a function of tibiofemoral geometry in healthy adults; and 2) quantifying the effect of tibiofemoral geometry on musculoskeletal function.

Methods

We used motion data for six activity types and CT images of the knee from 12 healthy adults. Geometrical variation of the tibia and femoral articular surfaces were measured in the CT images. The geometry-based tibiofemoral motion was calculated by fitting a parallel mechanism to geometrical variation in the cohort. Matched musculoskeletal models embedding the geometry-based tibiofemoral joint motion and a common generic tibiofemoral motion of reference were generated and used to calculate joint angles, net joint moments, muscle and joint forces for the six activities analysed. The tibiofemoral model was validated against bi-planar fluoroscopy measurements for walking for all the six planes of motion. The effect of tibiofemoral geometry on musculoskeletal function was the difference between the geometry-based model and the model of reference.

Results

1 The geometry-based tibiofemoral motion described the pattern and the variation
2 during walking for all six motion components, except the pattern of anterior tibial
3 translation. Tibiofemoral geometry had moderate effect on cohort-averages of
4 musculoskeletal function ($R^2 = 0.60 - 1$), although its effect was high in specific
5 instances of the model, outputs and activities analysed, reaching 2.94 BW for the
6 ankle reaction force during stair descent. In conclusion, tibiofemoral geometry is a
7 major determinant of tibiofemoral motion during walking.
8
9
10
11
12
13
14
15
16

17 **Significance**

18 Geometrical variations of the tibiofemoral joint are important for studying
19 musculoskeletal function during normal activity in specific individuals but not for
20 studying cohort averages of musculoskeletal function. This finding expands current
21 knowledge of movement biomechanics.
22
23
24
25
26
27
28
29
30
31
32
33
34
35
36
37
38
39
40
41
42
43
44
45
46
47
48
49
50
51
52
53
54
55
56
57
58
59
60
61
62
63
64
65

1. Introduction

1
2
3 Joint angles, net moments, and musculoskeletal forces are commonly calculated
4
5 by assuming a generic model of tibiofemoral motion adapted to each participant in a
6
7 variety of clinical and research settings [1]. However, the natural motion of the
8
9 tibiofemoral joint is three-dimensional, activity-dependent, and varies across
10
11 participants, determined by the complex interactions between the ligaments,
12
13 articulating surfaces of the bones and the load transmitted by the knee [2,3]. Thus,
14
15 quantifying how variations in tibiofemoral geometry affect calculations of
16
17 musculoskeletal function is important to both researchers and clinicians interested in
18
19 movement biomechanics.
20
21
22
23

24
25 During passive flexion-extension movements of the knee, tibiofemoral motion is
26
27 three-dimensional and highly reproducible [3]. Smoger et al. (2015) showed that
28
29 knee size and condylar geometry determine anterior–posterior tibiofemoral
30
31 translation, while Ottoboni et al. (2010) used ligament and articular surface geometry
32
33 to accurately model the three-dimensional tibiofemoral motion during passive knee
34
35 flexion [5]. Normal walking and non-weight-bearing knee flexion exercises induce,
36
37 respectively, 3.1 ± 2.4 mm and 2.6 ± 2.1 mm of anterior tibial translation [2].
38
39 Therefore, it appears that tibiofemoral motion during less strenuous activities like
40
41 walking may be largely attributable to tibiofemoral geometry. Yet, the distinct effects
42
43 of knee geometry and elasticity on musculoskeletal function is yet unclear.
44
45
46
47

48
49 Musculoskeletal modelling is finding increasing use in both clinical and research
50
51 settings [1]. The range of applications is broad, ranging from studies of fetal
52
53 development [6], femoral neck mechanics [7] , human motion [8] and knee
54
55 mechanics [9], and focuses both on personalized [10] and cohort averages of
56
57 different parameters of musculoskeletal function such as joint motion and muscle
58
59
60
61

1 forces, either for selected tasks or multiple activities [7,11,12]. Such a variety of
2 applications and objectives commonly requires a compromise between accuracy and
3 complexity in each specific application.
4

5
6
7 Compliant tibiofemoral joint models provide an elastic, load-dependent,
8 representation of tibiofemoral motion and typically require complex model generation
9 and solution processes [9,10]. For example, Navacchia and co-workers (2019) used
10 knee geometry extracted from both CT and MRI images and ligament material
11 properties calibrated to in vitro laxity tests to iteratively solve the tibiofemoral elastic
12 and motion problem in 76 – 210 minutes for two participants executing a single stride
13 and chair rise cycle. In contrast, rigid tibiofemoral joint models provide a load-
14 independent representation of tibiofemoral motion and are therefore exclusively
15 based on geometry. Rigid modelling enables computationally efficient analyses for
16 large cohorts, multiple activities and repeated tasks [8,11,13–15]. Most often, a
17 generic musculoskeletal model is scaled to each participant using measurements of
18 inter-segmental lengths [16]. On some occasions tibiofemoral motion is represented
19 by simple revolute, planar and spherical joint models [8,14]. On other occasions,
20 tibiofemoral motion is modelled by more complex articulated joint mechanisms
21 explicitly imposing the consistency between tibiofemoral motion, articular surface
22 and ligament geometry [17,18]. However, no study has compared the tibiofemoral
23 motion in the model against corresponding measurements obtained during normal
24 physical activity.
25
26
27
28
29
30
31
32
33
34
35
36
37
38
39
40
41
42
43
44
45
46
47
48
49
50

51 Here, we hypothesise that variation of tibiofemoral articular surface and ligament
52 geometry determine variation of tibiofemoral motion and musculoskeletal function.
53 To test this hypothesis, we aimed at 1) modelling the variation of tibiofemoral motion
54 exclusively using variations of tibiofemoral geometry in healthy adults; and 2)
55
56
57
58
59
60
61
62
63
64
65

1 studying the effect of geometrical variation of tibiofemoral motion on musculoskeletal
2 function. The geometry-based tibiofemoral motion was modelled by prescribing the
3 consistency between the tibiofemoral motion, the articular surface and the ligament
4 geometry. The variation of the geometry-based tibiofemoral motion was obtained by
5 embedding in the model variations of knee size in one cohort and validated against
6 corresponding bi-planar fluoroscopy measurements of all the six motion components
7 obtained in a second independent cohort [19]. The effect of tibiofemoral geometry on
8 musculoskeletal function was studied by comparing matched musculoskeletal
9 models embedding the geometry-based tibiofemoral motion and a common generic
10 tibiofemoral joint model of reference. Geometry-based and scaled-generic joint
11 angles, net moments, muscle and joint forces for six different normal activity types
12 were calculated and compared.
13
14
15
16
17
18
19
20
21
22
23
24
25
26
27
28
29
30
31

32 **2. Materials and Methods**

33 *2.1 Imaging and motion data*

34
35 Computed-Tomography (CT) images and motion data for one cohort of 12
36 healthy participants (females, age: 67 ± 5 years, weight: 75 ± 14 kg, height: 159 ± 7
37 cm) were obtained from our earlier work [7,20]. In summary, CT images of the distal
38 femur and the proximal tibia were obtained using a clinical whole-body scanner
39 (Aquilon CT, Toshiba Corporation, Tokyo). Motion data were comprised of
40 trajectories of 46 skin-mounted reflective markers and ground reaction forces. The
41 motion data were recorded for a static pose, normal walking, fast walking, jumping,
42 stair ascent, stair descent, rising from and sitting down onto a chair. Full details of
43 the marker set were reported by Dorn et al. (2012) [21].
44
45
46
47
48
49
50
51
52
53
54
55
56
57
58
59
60
61
62
63
64
65

2.2 *Dynamic bi-planar fluoroscopy measurements of tibiofemoral motion*

1
2
3
4
5
6
7
8
9
10
11
12
13
14
15
16
17
18
19
20
21
22
23
24
25
26
27
28
29
30
31
32
33
34
35
36
37
38
39
40
41
42
43
44
45
46
47
48
49
50
51
52
53
54
55
56
57
58
59
60
61
62
63
64
65

Mobile bi-plane fluoroscopy measurements of tibiofemoral joint motion while walking (1.03 – 1.51 m/s) were obtained for a second independent cohort by Gray et al. (2019). The cohort comprised fifteen healthy individuals (age: 31 ± 6 years, weight: 67 ± 8 kg, height: 168 ± 9 cm) with no knee pain and history of knee surgery [19]. The study provided mean and standard deviation for all six motion components in the tibiofemoral coordinate system by Grood and Suntay (1983) [22].

2.3 *Scaled-generic musculoskeletal modelling*

Full-body scaled-generic musculoskeletal models were obtained earlier [7,14] by scaling the generic model described by Dorn et al. (2012)[21], an evolution of the generic model 'gait2392' provided with OpenSim embedding the planar tibiofemoral joint motion created by Yamaguchi and Zajac (1989)[23]. The generic model was fitted to each participant's mass and inter-segment distances using OpenSim's built-in scaling function [16]. The tibiofemoral motion was scaled to the participants using the distance between the anterior superior iliac spine and the lateral epicondyles (thigh length). The validity of the model was assessed by comparing joint and muscle forces in the model to corresponding published measurements [7,14].

2.4 *Geometry-based musculoskeletal modelling*

The variation of tibiofemoral geometry in the cohort was described by scaling a baseline anatomy to match width and depth of both the femoral and tibial bones because size differences largely explain the variation of tibiofemoral motion in healthy adults [4]. The baseline anatomy included the bone surfaces of the tibia and the femur, the cartilaginous articular surfaces and ligament insertions (Anterior Cruciate Ligament, ACL; Posterior Cruciate Ligament, PCL; Medial Collateral

1 Ligament, MCL) from a healthy male donor (height: 173 cm; mass: 61.2 kg). The
2 proximal tibia and distal femur in the participants were segmented from the CT
3 images (ScanIP, Simpleware, Exeter, UK). The width and depth of tibial and femoral
4 condyles were measured from the segmented bone geometries. Antero-posterior
5 and medio-lateral scaling factors were determined by scaling the baseline bone
6 geometry to the width and depth of the tibia and the femur in the participants (Table
7 S6). The articular surfaces of the cartilage, the ligaments origin and insertion in the
8 baseline anatomy were then scaled to each participant. Anatomical reference
9 systems were created for the tibia and femur using the skeletal surfaces [24]
10 assuming the tibia longitudinal axis coincident with the longitudinal axis in the images
11 because the distal tibia was not available (Figure 1).
12
13
14
15
16
17
18
19
20
21
22
23
24
25
26

27 The geometry-based tibiofemoral motion was calculated using a parallel
28 mechanism. The procedure was described and validated earlier against
29 experimental measurement for all six motion components by Conconi et al.
30 (2018)[25]. The geometry-based tibiofemoral joint motion was determined by
31 prescribing uniform ligament lengths and continuous contact of the articular surfaces
32 over 120° of knee flexion [25]. Firstly, the tibiofemoral joint motion was estimated by
33 minimizing a geometrical estimator of the peak contact pressure over intermediate
34 knee flexion angles [26,27]. Next, a single-degree-of-freedom spatial parallel
35 mechanism was generated composed of the femur and tibia connected by five struts.
36 Three of the five struts were defined using the attachment sites of the ACL, PCL and
37 MCL. The remaining two struts were defined using the curvature of the femoral and
38 tibial condyles. Finally, the spatial linkage was synthesized by optimizing the
39 coordinates of the ligaments' attachment points and the lengths of the five struts
40
41
42
43
44
45
46
47
48
49
50
51
52
53
54
55
56
57
58
59
60
61
62
63
64
65

1 within a 2 mm variation to best match the initial estimate of tibiofemoral joint motion
2 [24] (Figure 1).
3

4 The geometry-based tibiofemoral pose was calculated using the spatial linkage at
5 2° intervals between 0° and 120° knee flexion. Then, the tibiofemoral pose was
6 decomposed into translations and Euler angles (i.e., tibiofemoral abduction, flexion
7 and external rotation). The tibiofemoral pose in the CT images was assumed 0° of
8 knee flexion. The geometry-based musculoskeletal model was obtained by
9 duplicating the scaled-generic model and by implementing the geometry-based
10 tibiofemoral motion using a custom joint in OpenSim. The parent (femur) coordinate
11 system in the geometry-based tibiofemoral joint model was aligned to the parent
12 coordinate system in the scaled-generic knee model. Tibiofemoral joint translations
13 and rotations were expressed as a function of the knee flexion angle using cubic
14 splines. The hip-to-knee and knee-to-ankle distances were matched to those in the
15 scaled-generic model to ensure identical leg lengths in both models at zero knee
16 flexion (Figure 1).
17
18
19
20
21
22
23
24
25
26
27
28
29
30
31
32
33
34
35

36 The geometry-based musculoskeletal function for normal walking, fast walking,
37 jumping, stair ascent, stair descent, rising from and sitting down onto a chair was
38 calculated using the same inverse kinematic and static optimization procedures used
39 earlier for the scaled-generic models [7,20].
40
41
42
43
44
45
46
47
48

49 *2.5 Data analysis*

50 The six motion components while walking in geometry-based and scaled-generic
51 models generated for the first cohort was compared to corresponding measurements
52 in the second independent cohort of healthy adults (aim 1).
53
54
55
56
57
58
59
60
61
62
63
64
65

1
2
3
4
5
6
7
8
9
10
11
12
13
14
15
16
17
18
19
20
21
22
23
24
25
26
27
28
29
30
31
32
33
34
35
36
37
38
39
40
41
42
43
44
45
46
47
48
49
50
51
52
53
54
55
56
57
58
59
60
61
62
63
64
65

The effect of tibiofemoral geometry on musculoskeletal function (aim 2) was the difference between geometry-based and scaled-generic outputs. Muscle and joint reaction forces were normalized by participants' body weight (BW). Joint angles, net joint moments, muscle forces and joint reaction forces in different participants and activities were pooled and analysed using linear regression analysis. Average and peak differences were assessed using the Root Mean Square Error (RMSE) and the 98th percentile of the difference distribution. Percentage differences were calculated using the scaled-generic range of joint angles, peak net joint moments, peak muscle forces, and peak joint reaction forces across activities.

3. Results

Consistent with Gray et al. (2019), the geometry-based tibiofemoral joint while walking was slightly bent ($1^{\circ} - 12^{\circ}$) at heel-strike, reached its maximum flexion ($9^{\circ} - 23^{\circ}$) at contralateral toe-off (CTO) and then extended to a minimum flexion angle ($0^{\circ} - 9^{\circ}$) before rapidly flexing to $63^{\circ} - 70^{\circ}$ knee flexion at 70% gait cycle (Figure 2A). The knee abduction angle ($-7 - -2^{\circ}$) and distraction ($-4 - 0$ mm) showed relatively small changes over the gait cycle. The range of knee external rotation was $-8^{\circ} - 7^{\circ}$ during stance and reached the peak internal rotation at peak knee flexion during swing ($0^{\circ} - 13^{\circ}$). The knee lateral translation showed modest changes during stance ($-1.5 - 3.5$ mm) before translating medially during late stance and early swing ($-3.2 - 2.0$ mm). Also consistent with the reference measurements was the variation across participants of the tibial anterior translation (± 2.5 mm). However, the pattern of the tibial anterior translation did not capture the anterior shift observed between heel strike and contralateral toe-off ($2.7 - 2.8$ mm) and during early swing (5.3 mm). Also,

1 the range of tibiofemoral flexion (63° on average) was smaller than that in the
2 fluoroscopy measurements (68° on average).
3

4 The scaled-generic and geometry-based tibiofemoral flexion angle were
5 practically identical ($R^2 = 1$) (Figure 2B) and both provided comparable patterns for
6 the remaining 5 motion components, except for 8 mm anterior translation offset and
7 increased scaled-generic anterior translation and distraction during swing. However,
8 the variance in the scaled-generic tibiofemoral motion was smaller than that in the
9 fluoroscopy measurements for tibia anterior translation and distraction (0.9 mm and
10 0.7 mm) and zero for tibiofemoral abduction, external rotation and lateral translation,
11 as prescribed in the tibiofemoral model of reference.
12
13
14
15
16
17
18
19
20
21
22
23

24 The effect of variation of tibiofemoral geometry on musculoskeletal function was
25 modest in cohort averages of all the musculoskeletal outputs (Figures 3 – 7). When
26 all results were pooled, the range of the coefficient of determination between scaled-
27 generic and geometry-based model outputs was 0.60 – 1 in overall (Figures 3 – 5).
28 Average differences in hip, knee and ankle angles were less than 0.5 – 4.0° and
29 peak difference reached 14° for the hip rotation (29.5%) (Figure 3). Average
30 differences in net joint moments were 0.6 – 4.2 Nm while peak differences reached
31 20.4 Nm at the knee (32.7%) (Figure 4). Average differences in joint reaction forces
32 were 0.37 – 0.47 BW and peak differences reached 1.3 – 2.1 BW (30 – 36%) (Figure
33 5). Average difference in muscle forces were 0 – 0.26 BW and the peak difference
34 was 0.01 – 1.00 BW (Figure 6 – 7).
35
36
37
38
39
40
41
42
43
44
45
46
47
48
49
50

51 By pooling the results activity-by-activity, the peak difference between scaled-
52 generic and geometry-based joint angles was less than 1° across activities and
53 joints. Net joint moment varied by less than 1.7 Nm for all activities and joints, except
54 for 6.3 Nm difference found at the ankle between normal walking and rising from and
55
56
57
58
59
60
61
62
63
64
65

1 sitting on a chair. Joint reaction forces varied from 0.31 – 0.58 BW for walking to
2 1.77 – 2.94 BW for stair descent. Muscle forces varied from 0.01 – 0.36 BW for
3 walking to 0 – 2.45 BW for jumping (Table S2 – S5, Supplementary Material).
4
5
6
7
8
9

10 **4. DISCUSSION**

11 We hypothesised that variation of tibiofemoral geometry determines variations in
12 tibiofemoral motion and musculoskeletal function. We calculated a geometry-based
13 tibiofemoral motion exclusively based on variation of tibiofemoral geometry in a
14 cohort of healthy adults and compared the calculated motion to corresponding
15 fluoroscopy measurements for all six planes of motion in a second independent
16 cohort (aim 1). The effect of tibiofemoral geometry on musculoskeletal was studied
17 by comparing matched musculoskeletal models embedding the geometry-based and
18 a generic tibiofemoral motion. We found that 1) the tibiofemoral geometry variation is
19 the major determinant of tibiofemoral motion during walking in healthy adults; and 2)
20 the tibiofemoral geometry variation has moderate effect on cohort averages of
21 musculoskeletal function and large effect on musculoskeletal function for individual
22 instances of the cohort, particularly when muscle and joint forces are of interest.
23
24
25
26
27
28
29
30
31
32
33
34
35
36
37
38
39
40
41

42 Variation of tibiofemoral geometry is a major determinant of tibiofemoral motion in
43 healthy adults during normal activity because the tibiofemoral motion determined
44 exclusively using geometrical information of the tibiofemoral joint described most of
45 the variation in corresponding fluoroscopy measurements during walking. The major
46 differences included the smaller range of knee flexion attributable to the age
47 difference between the present cohort (age: 67 ± 5) and the younger cohort (31 ± 6
48 years) that provided the fluoroscopy measurements [28]. Also, the geometry-based
49 tibiofemoral motion did not capture the anterior tibial shift during early stance (2.7 –
50
51
52
53
54
55
56
57
58
59
60
61
62
63
64
65

1 2.8 mm) and early swing (5.3 mm; 60 – 80% gait) in the fluoroscopy measurements
2 (Figure 2A), which may be partially attributed to the knee compliance not included in
3 the model. Nevertheless, the geometry-based tibiofemoral motion displayed similar
4 variation to corresponding fluoroscopy measurements for all the six motion
5 components and similar pattern for five motion components, hence supporting our
6 hypothesis that tibiofemoral geometry determines tibiofemoral motion during normal
7 activity. This finding is in line with the association between articular surface geometry
8 and tibiofemoral motion during squatting exercises reported by Smoger et al. (2015)
9 [4] and it expands its validity to the geometry of the ligaments, and to walking.

10 The scaled-generic tibiofemoral motion provided a valid reference for studying
11 the effect of tibiofemoral geometry on musculoskeletal function. In fact, the scaled-
12 generic tibiofemoral motion showed consistent pattern but smaller variance in all the
13 secondary planes of motion as compared to corresponding fluoroscopy
14 measurements. We found that variation of tibiofemoral geometry affects moderately
15 cohort averages of musculoskeletal function across all the musculoskeletal outputs
16 analysed ($R^2 = 0.60 - 1$). The size of the cohort used in this study ($n=12$) appears
17 adequate for studying cohort averages of every musculoskeletal model output
18 including muscle forces, which were most sensitive to changes in tibiofemoral motion
19 (Figure 6 and Figure S1). Scaled-generic models are therefore valid and efficient
20 solutions for determining, for example, the main effect of a clinical intervention [29].
21 Nevertheless, variation of tibiofemoral geometry had a non-negligible effect in
22 individual instances of the model causing variation of musculoskeletal function
23 reaching 1 – 2.45 BW for muscle and joint forces. This finding is consistent with the
24 notion that consistency between tibiofemoral geometry and motion is important in the
25
26
27
28
29
30
31
32
33
34
35
36
37
38
39
40
41
42
43
44
45
46
47
48
49
50
51
52
53
54
55
56
57
58
59
60
61
62
63
64
65

1 context of personalized applications (within participant), particularly for studying
2 muscle and joint forces [9].
3

4 The consistency between the geometry-based tibiofemoral joint motion calculated
5 here and corresponding measurements obtained in vivo [19] is in line with earlier
6 validation studies showing that the parallel mechanism used here can provide an
7 accurate representation of tibiofemoral motion in a single participant [30] and four
8 knee specimens [5,24]. The present study demonstrates the robustness of the
9 method for a cohort of healthy participants for which only the skeletal geometry is
10 available for studying cohort-based variation of tibiofemoral motion. Yet, the validity
11 of the present modelling procedure for studying personalized musculoskeletal
12 function remains unclear because no bi-planar fluoroscopy measurements of
13 tibiofemoral motion were available for the present cohort. The effect of geometrical
14 variations of the tibiofemoral joint on the hip joint force reported here is similar to that
15 caused by anatomical errors committed while scaling a generic musculoskeletal
16 model to a specific participant (0.2 – 0.7 BW) [20,31] and smaller than that caused
17 by skin-motion artefacts (1.5 – 1.8 BW) [32] and potentially caused by muscle co-
18 contraction (8 – 10 BW) [13]. Therefore, it appears that studying personalized
19 features of musculoskeletal function requires accurate information of every
20 anatomical and functional parameter in the model, including tibiofemoral joint motion.
21
22
23
24
25
26
27
28
29
30
31
32
33
34
35
36
37
38
39
40
41
42
43
44

45 One limitation of the present study is the rigid tibiofemoral motion assumption that
46 prevents studying tibiofemoral motion changes in functional tasks of variable
47 demand. Nevertheless, our aim was to examine the independent effect of
48 tibiofemoral geometry. The present results are relevant to a broad range of
49 applications of rigid-body modelling [8,11,13–15]. The spatial linkage described here
50 can be extended to account for the elasticity of each ligament [33] or their lumped
51
52
53
54
55
56
57
58
59
60
61
62
63
64
65

1 effect into a single knee compliance matrix [34], hence potentially providing an
2 alternative solution to current methods for modelling the knee joint compliance [9,10].
3
4 Finally, the effect of tibiofemoral geometry on musculoskeletal function reported here
5 was determined using as reference a common generic tibiofemoral model [23]
6 scaled to the cohort using marker-based measurements of thigh length. Other
7 generic tibiofemoral models [35] and methods for fitting a generic musculoskeletal
8 model to the participant [36] may provide a valid alternative to the scaled-generic
9 model used here. However, the scaled-generic model used here provided a common
10 and valid motion of reference for isolating the effect of tibiofemoral geometry on
11 musculoskeletal function.
12
13
14
15
16
17
18
19
20
21
22
23

24 In conclusion, tibiofemoral motion during walking is mostly determined by
25 tibiofemoral geometry. Variation of tibiofemoral motion on musculoskeletal function is
26 on average modest, supporting the use of a generic tibiofemoral joint models for
27 studying the main effect of intervention in large cross-sectional studies.
28 Nevertheless, musculoskeletal function in specific individuals often requires
29 information of tibiofemoral geometry, particularly when estimates of muscle and joint
30 forces are of interest. The present findings expand knowledge of movement
31 biomechanics and can inform the decision-making process for modelling
32 musculoskeletal function.
33
34
35
36
37
38
39
40
41
42
43
44
45
46
47
48
49
50

51 **ACKNOWLEDGMENTS**

52 The Australian Research Council (DP180103146; FT180100338) and the State
53 Government of South Australia are gratefully acknowledged. The authors would also
54 thank Mr. Mark Williams for his contribution to coding.
55
56
57
58
59
60
61
62
63
64
65

1
2
3
4
5
6
7
8
9
10
11
12
13
14
15
16
17
18
19
20
21
22
23
24
25
26
27
28
29
30
31
32
33
34
35
36
37
38
39
40
41
42
43
44
45
46
47
48
49
50
51
52
53
54
55
56
57
58
59
60
61
62
63
64
65

REFERENCES

- [1] J.L. Hicks, T.K. Uchida, A. Seth, A. Rajagopal, S.L. Delp, Is my model good enough? Best practices for verification and validation of musculoskeletal models and simulations of movement., *J. Biomech. Eng.* 137 (2015) 020905. doi:10.1115/1.4029304.
- [2] C. a. Myers, M.R. Torry, K.B. Shelburne, J.E. Giphart, R.F. LaPrade, S.L.-Y. Woo, J.R. Steadman, In Vivo Tibiofemoral Kinematics During 4 Functional Tasks of Increasing Demand Using Biplane Fluoroscopy, *Am. J. Sports Med.* 40 (2012) 170–178. doi:10.1177/0363546511423746.
- [3] L. Blankevoort, R. Huiskes, A. De Lange, Helical axes of passive knee joint motions, *J. Biomech.* 23 (1990) 1219–1229. doi:10.1016/0021-9290(90)90379-H.
- [4] L.M. Smoger, C.K. Fitzpatrick, C.W. Clary, A.J. Cyr, L.P. Maletsky, P.J. Rullkoetter, P.J. Laz, Statistical modeling to characterize relationships between knee anatomy and kinematics, *J. Orthop. Res.* 33 (2015) 1620–1630. doi:10.1002/jor.22948.
- [5] A. Ottoboni, V. Parenti-Castelli, N. Sancisi, C. Belvedere, A. Leardini, Articular surface approximation in equivalent spatial parallel mechanism models of the human knee joint: An experiment-based assessment, *Proc. Inst. Mech. Eng. Part H J. Eng. Med.* 224 (2010) 1121–1132. doi:10.1243/09544119JEIM684.
- [6] S.W. Verbruggen, B. Kainz, S.C. Shelmerdine, O.J. Arthurs, J. V. Hajnal, M.A. Rutherford, A.T.M. Phillips, N.C. Nowlan, European Society of Biomechanics S.M. Perren Award 2018: Altered biomechanical stimulation of the developing hip joint in presence of hip dysplasia risk factors, *J. Biomech.* 78 (2018) 1–9. doi:10.1016/J.JBIOMECH.2018.07.016.
- [7] M.E. Kersh, S. Martelli, R.M.D. Zebaze, E. Seeman, M.G. Pandy, Mechanical Loading of the Femoral Neck in Human Locomotion., *J. Bone Miner. Res.* 33 (2018) 1999–2006. doi:10.1002/jbmr.3529.
- [8] R. Dumas, F. Moissenet, X. Gasparutto, L. Cheze, Influence of joint models on lower-limb musculo-tendon forces and three- dimensional joint reaction forces during gait, *Spec. Issue Artic. Proc IMechE Part H J Eng. Med.* 226 (2012) 146–160. doi:10.1177/0954411911431396.
- [9] P. Gerus, M. Sartori, T.F. Besier, B.J. Fregly, S.L. Delp, S.A. Banks, M.G. Pandy, D.D. D’Lima, D.G. Lloyd, Subject-specific knee joint geometry improves predictions of medial tibiofemoral contact forces., *J. Biomech.* 46 (2013) 2778–86. doi:10.1016/j.jbiomech.2013.09.005.
- [10] A. Navacchia, D.R. Hume, P.J. Rullkoetter, K.B. Shelburne, A computationally efficient strategy to estimate muscle forces in a finite element musculoskeletal model of the lower limb, *J. Biomech.* 84 (2019) 94–102. doi:10.1016/J.JBIOMECH.2018.12.020.
- [11] H. Ziaei-poor, M. Taylor, M. Pandy, S. Martelli, A novel training-free method for real-time prediction of femoral strain, *J. Biomech.* 86 (2019) 110–116. doi:10.1016/J.JBIOMECH.2019.01.057.
- [12] H. Ziaei-poor, S. Martelli, M.G. Pandy, M. Taylor, Efficacy and efficiency of multivariate linear regression for the rapid prediction of the femoral strain field during activity, *Med. Eng. Phys.* 63 (2019) 88–92. doi:10.1016/j.medengphy.2018.12.001.
- [13] S. Martelli, D. Calvetti, E. Somersalo, M. Viceconti, Stochastic modelling of

- muscle recruitment during activity, *Interface Focus*. 5 (2015) 20140094-.
doi:10.1098/rsfs.2014.0094.
- [14] S. Martelli, G. Valente, M. Viceconti, F. Taddei, Sensitivity of a subject-specific musculoskeletal model to the uncertainties on the joint axes location., *Comput. Methods Biomech. Biomed. Engin.* 18 (2015) 1555–63.
doi:10.1080/10255842.2014.930134.
- [15] E.M. Arnold, S.R. Ward, R.L. Lieber, S.L. Delp, A model of the lower limb for analysis of human movement., *Ann. Biomed. Eng.* 38 (2010) 269–79.
doi:10.1007/s10439-009-9852-5.
- [16] S.L. Delp, F.C. Anderson, A.S. Arnold, P. Loan, A. Habib, C.T. John, E. Guendelman, D.G. Thelen, OpenSim: open-source software to create and analyze dynamic simulations of movement, *IEEE Trans. Biomed. Eng.* 54 (2007) 1940–1950. doi:10.1109/TBME.2007.901024.
- [17] M. Barzan, L. Modenese, C.P. Carty, S. Maine, C.A. Stockton, N. Sancisi, A. Lewis, J. Grant, D.G. Lloyd, S. Brito da Luz, Development and validation of subject-specific pediatric multibody knee kinematic models with ligamentous constraints, *J. Biomech.* 93 (2019) 194–203.
doi:10.1016/j.jbiomech.2019.07.001.
- [18] S. Brito da Luz, L. Modenese, N. Sancisi, P.M. Mills, B. Kennedy, B.R. Beck, D.G. Lloyd, Feasibility of using MRIs to create subject-specific parallel-mechanism joint models, *J. Biomech.* 53 (2017) 45–55.
doi:10.1016/j.jbiomech.2016.12.018.
- [19] H.A. Gray, S. Guan, L.T. Thomeer, A.G. Schache, R. de Steiger, M.G. Pandy, Three-dimensional motion of the knee-joint complex during normal walking revealed by mobile biplane x-ray imaging, *J. Orthop. Res.* 37 (2019) 615–630.
doi:10.1002/jor.24226.
- [20] S. Martelli, M.E. Kersh, M.G. Pandy, Sensitivity of femoral strain calculations to anatomical scaling errors in musculoskeletal models of movement, *J. Biomech.* 48 (2015) 3615–24. doi:10.1016/j.jbiomech.2015.08.001.
- [21] T.W. Dorn, A.G. Schache, M.G. Pandy, Muscular strategy shift in human running: dependence of running speed on hip and ankle muscle performance., *J. Exp. Biol.* 215 (2012) 1944–56. doi:10.1242/jeb.064527.
- [22] E.S. Grood, W.J. Suntay, A joint coordinate system for the clinical description of three-dimensional motions: application to the knee, *J. Biomech. Eng.* 105 (1983) 136–144.
- [23] G.T. Yamaguchi, F.E. Zajac, A planar model of the knee joint to characterize the knee extensor mechanism, *J. Biomech.* 22 (1989) 1–10.
- [24] N. Sancisi, V. Parenti-Castelli, A novel 3D parallel mechanism for the passive motion simulation of the patella-femur-tibia complex, *Meccanica*. 46 (2011) 207–220. doi:10.1007/s11012-010-9405-x.
- [25] M. Conconi, N. Sancisi, V. Parenti-Castelli, Subject-Specific Model of Knee Natural Motion: A Non-invasive Approach, in: *Proc. Adv. Robot.*, Springer, Cham, 2018: pp. 255–264. doi:10.1007/978-3-319-56802-7_27.
- [26] M. Conconi, A. Leardini, V. Parenti-Castelli, Joint kinematics from functional adaptation: A validation on the tibio-talar articulation, *J. Biomech.* 48 (2015) 2960–2967. doi:10.1016/j.jbiomech.2015.07.042.
- [27] M. Conconi, V. Parenti-Castelli, A sound and efficient measure of joint congruence, *Proc. Inst. Mech. Eng. Part H J. Eng. Med.* 228 (2014) 935–941.
doi:10.1177/0954411914550848.
- [28] J. Favre, J.C. Erhart-Hledik, T.P. Andriacchi, Age-related differences in

- sagittal-plane knee function at heel-strike of walking are increased in osteoarthritic patients, *Osteoarthr. Cartil.* 22 (2014) 464–471. doi:10.1016/J.JOCA.2013.12.014.
- [29] N.S. Thompson, R.J. Baker, A.P. Cosgrove, I.S. Corry, H.K. Graham, Musculoskeletal modelling in determining the effect of botulinum toxin on the hamstrings of patients with crouch gait., *Dev. Med. Child Neurol.* 40 (1998) 622–5. doi:10.1111/j.1469-8749.1998.tb15428.x.
- [30] F. Nardini, N. Sancisi, C. Belvedere, M. Conconi, A. Leardini, V.P. Castelli, Definition of a subject-specific model of the knee in vivo, *Gait Posture.* 49 (2016) S6. doi:10.1016/j.gaitpost.2016.07.030.
- [31] G. Lenaerts, W. Bartels, F. Gelaude, M. Mulier, A. Spaepen, G. Van der Perre, I. Jonkers, Subject-specific hip geometry and hip joint centre location affects calculated contact forces at the hip during gait, *J. Biomech.* 42 (2009) 1246–1251.
- [32] G. Lamberto, S. Martelli, A. Cappozzo, C. Mazzà, To what extent is joint and muscle mechanics predicted by musculoskeletal models sensitive to soft tissue artefacts?, *J. Biomech.* 62 (2016) 68–76. doi:10.1016/j.jbiomech.2016.07.042.
- [33] N. Sancisi, V. Parenti-Castelli, A sequentially-defined stiffness model of the knee, *Mech. Mach. Theory.* 46 (2011) 1920–1928. doi:10.1016/j.mechmachtheory.2011.07.006.
- [34] G. Lamberto, D.B. Amin, L.B. Solomon, B. Ding, K.J. Reynolds, C. Mazzà, S. Martelli, Personalised 3D knee compliance from clinically viable knee laxity measurements: A proof of concept ex vivo experiment, *Med. Eng. Phys.* 64 (2018) 80–85. doi:10.1016/J.MEDENGGPHY.2018.12.003.
- [35] P.S. Walker, J.S. Rovick, D.D. Robertson, The effects of knee brace hinge design and placement on joint mechanics, *J. Biomech.* 21 (1988). doi:10.1016/0021-9290(88)90135-2.
- [36] J. Zhang, H. Sorby, J. Clement, C.D.L. Thomas, P. Hunter, P. Nielsen, D. Lloyd, M. Taylor, T. Besier, The MAP Client: User-Friendly Musculoskeletal Modelling Workflows, in: Springer International Publishing, 2014: pp. 182–192. doi:10.1007/978-3-319-12057-7_21.

1

FIGURES

2 Figure 1 –The process involved segmentation of the CT images (A), bi-axial scaling
3 (transversal plane) of the template geometry (B), calculation of the geometry-based
4 tibiofemoral motion by imposing the consistency between the motion and the geometry
5 of the ACL, PCL, MCL and spherical approximations (shaded spheres) of femoral and
6 tibial condyles (C) and, substitution of the scaled-generic tibiofemoral motion in the
7 scaled-generic model using the geometry-based tibiofemoral motion (D). The distance
8 between the Right Anterior Superior Spine (RASIS) and the Lateral Epicondyle (LE)
9 displayed in the figure were used to scale the generic musculoskeletal model to each
10 participant.

11 Figure 2 – In figure 2A, the geometry-based tibiofemoral motion (shaded grey)
12 compared to corresponding bi-planar fluoroscopy measurements (shaded red) for
13 walking (mean \pm 1SD). The average standing position (solid black and red lines), the
14 heel-strike (HS), contralateral toe-off (CTO), contralateral heel-strike (CHS) and toe-
15 off (TO) events are also displayed. In figure 2B, the geometry-based (shaded grey)
16 and scaled-generic (shaded green) tibiofemoral motion (mean \pm 1SD) compared to
17 the mean fluoroscopy measurement (solid blue) in the OpenSim's knee coordinate
18 system. The two separate comparisons (Figure 2A and 2B) were necessary because
19 bi-planar fluoroscopy measurements for each individual participant were not available.

20 Figure 3 – Linear correlation analysis of scaled-generic and geometry-based joint
21 angles.

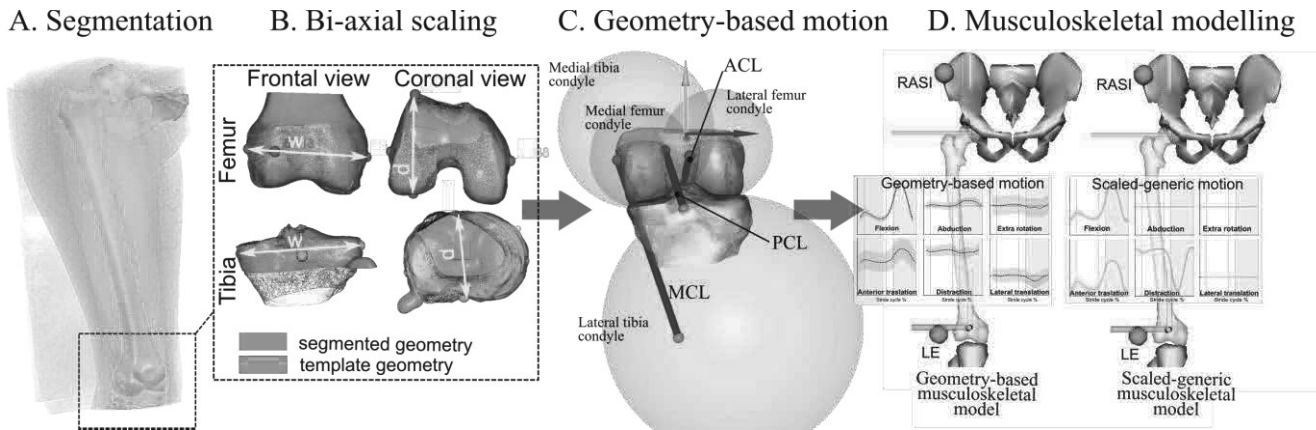
22 Figure 4 – Linear correlation analysis of scaled-generic and geometry-based joint
23 moments.

24 Figure 5 – Linear correlation analysis of scaled-generic and geometry-based joint
25 forces.

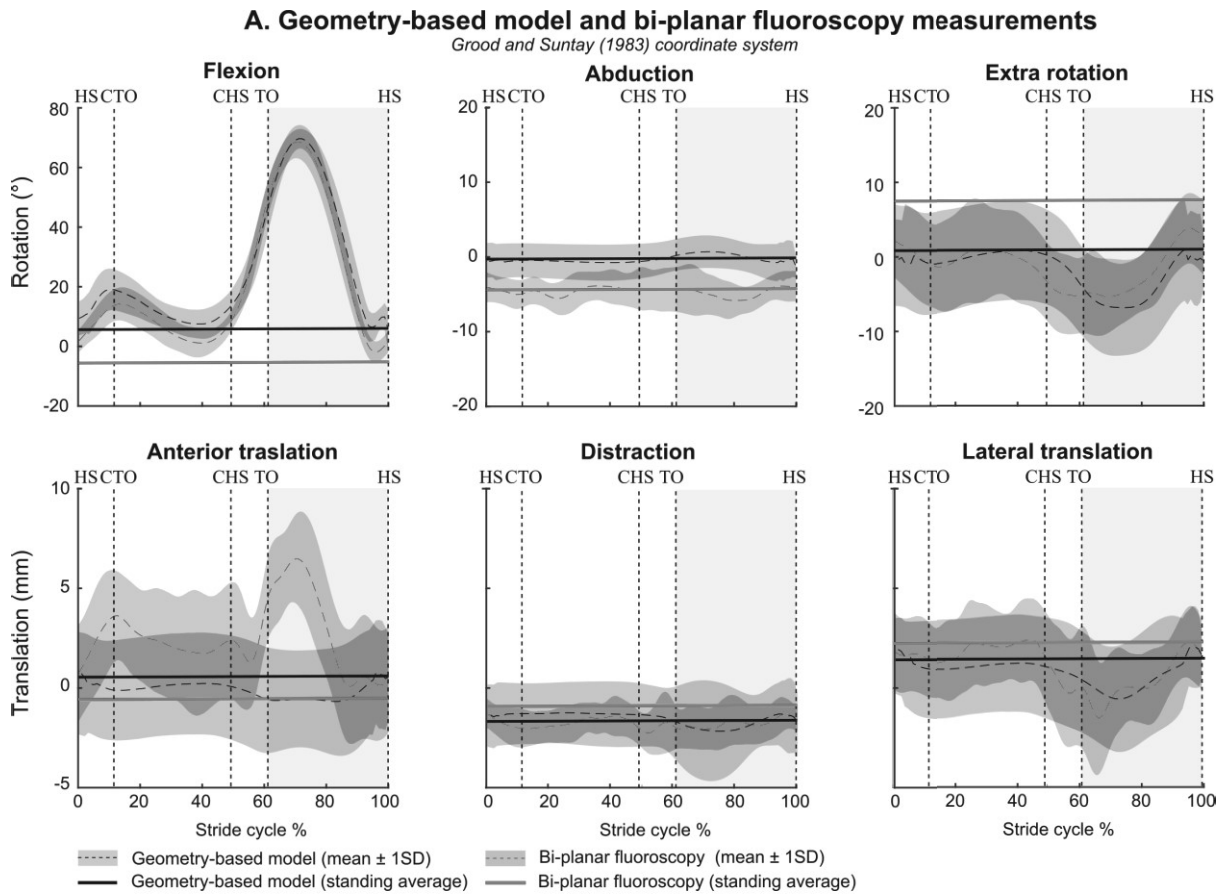
26 Figure 6 – Scaled-generic (red) and geometry-based (grey) muscle force time histories
27 during walking. The average muscle force pattern (solid line) and the one standard
28 deviation band (shaded region) are displayed.

29

30 **Figure 1**

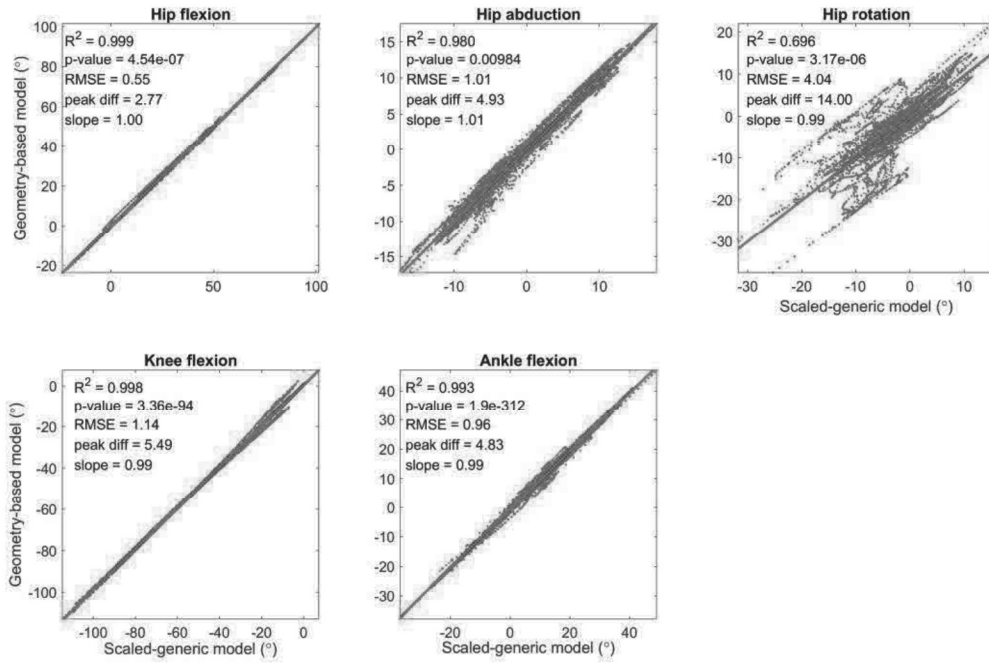


33 **Figure 2**



34

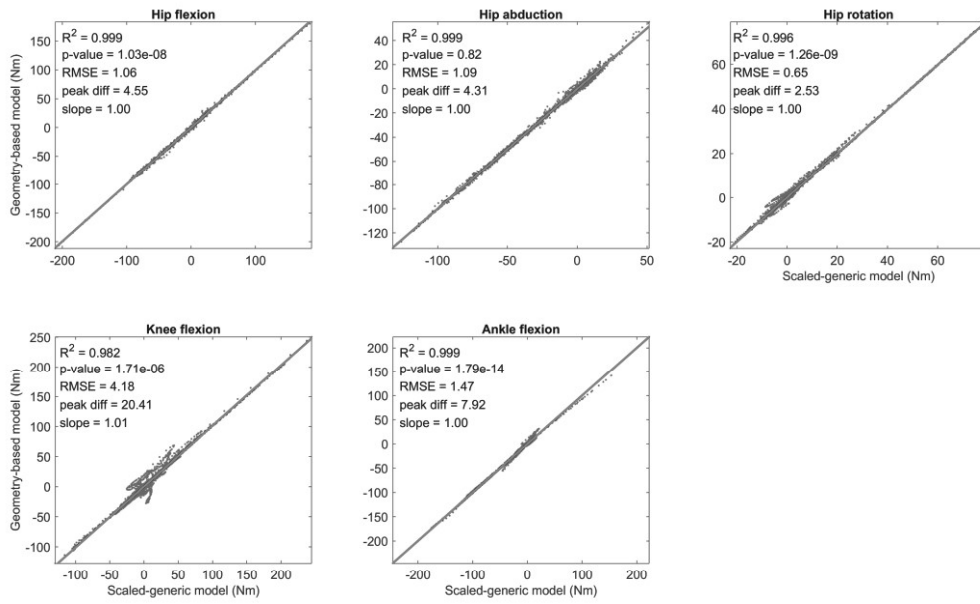
35 **Figure 3**



36

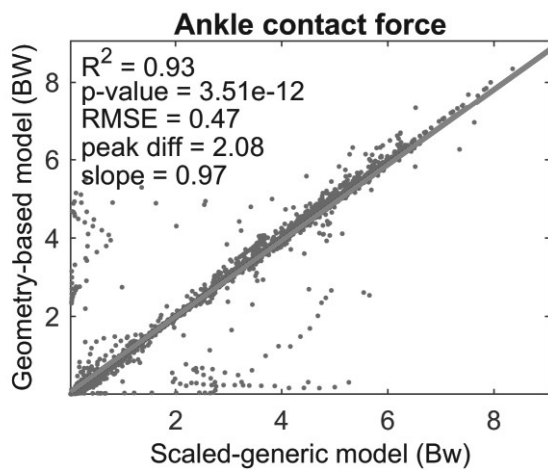
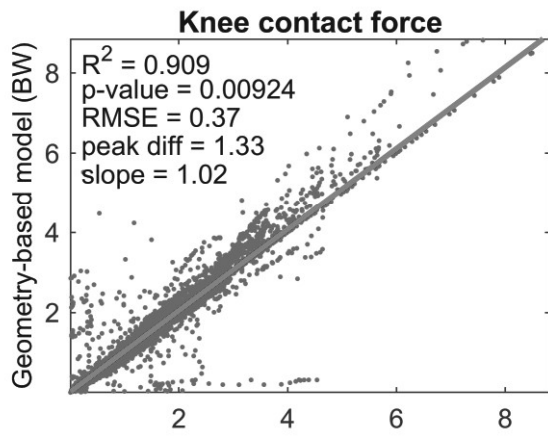
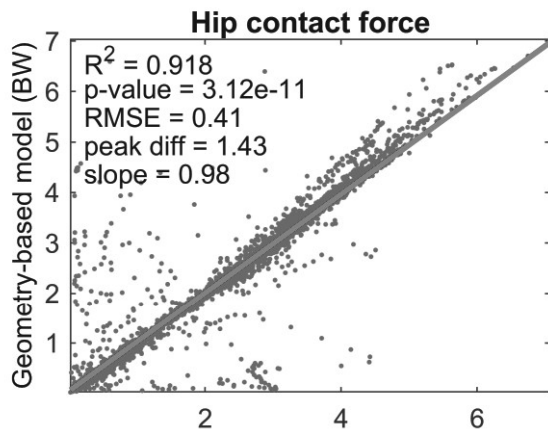
37

38 **Figure 4**



39

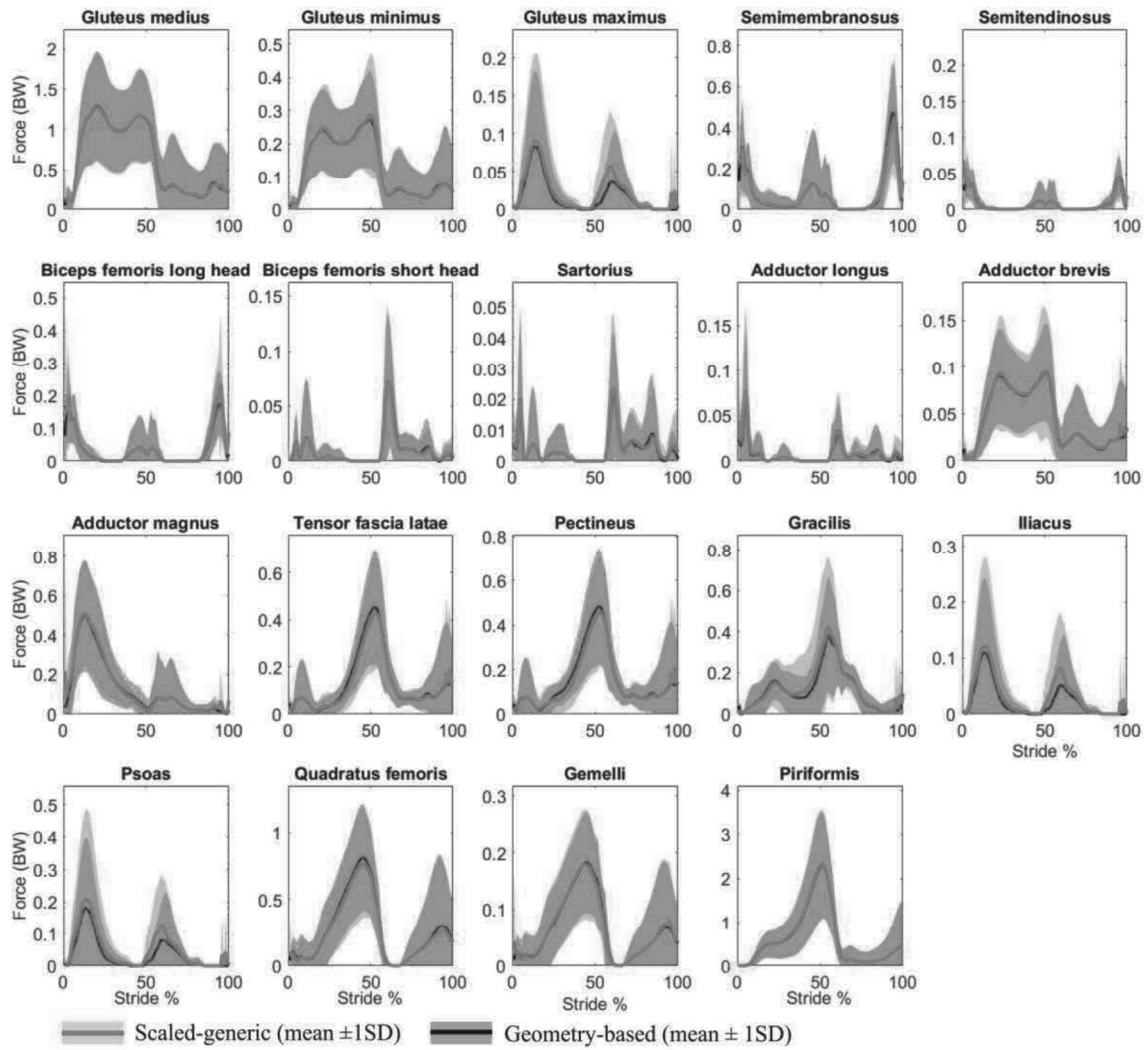
40 **Figure 5**



41

42

43 **Figure 6**



44

45

46